Z. Phys. Chem. **226** (2012) 665–674 / **DOI** 10.1524/zpch.2012.0294

Direct-Imaging Cryo-SEM of Nanostructure Evolution in Didodecyldimethylammonium Bromide-Based Microemulsions

By Ido Ben-Barak and Yeshayahu Talmon*

Department of Chemical Engineering, Technion – Israel Institute of Technology, Haifa 32000, Israel

Dedicated to Matthias Ballauff on the occasion of his 60th birthday

(Received June 9, 2012; accepted in revised form July 9, 2012)
(Published online August 13, 2012)

Nanostructure / Microemulsions / DDAB / Cryo-SEM

We applied cryogenic-temperature scanning electron microscopy (cryo-SEM) to perform a first direct-imaging study of single-phase microemulsions of didodecyldimethylammonium bromide (DDAB), isooctane, and water. The structural changes from a bicontinuous network to an oil-continuous structure, observed upon the addition of water to the system, are consistent with previous indirect investigations, thus validating the model of Ninham, Evans, and coworkers, published in 1984, and demonstrating the power of this novel methodology.

1. Introduction

Didodecyldimethylammonium bromide (DDAB) is a cationic double-tailed surfactant, each tail is a normal chain of 12 carbon atoms. When mixed with proper amounts of oil and water, this surfactant forms a single-phase ternary microemulsion [1]. Investigation of the properties of DDAB microemulsions goes to the core of microemulsion theory and practice, and has proven useful and applicable to the understanding and design of microemulsion properties, specifically the effect of a microemulsion components on its nanostructure and curvature [2,3].

Across the single-phase microemulsion region of the DDAB-oil-water phase diagram, unusual properties have been observed. For microemulsions of a fixed surfactant/oil ratio, systems of low water-content are electrically conductive, while the addition of water to the system leads a very sharp drop of electrical conductivity, rendering the solution practically nonconductive. This counterintuitive behavior, namely sharply decreased electrical conductivity upon addition of a conductive component, was observed for a series of oils with hydrocarbon chains up to twelve carbon atoms long. However, single-phase microemulsions containing longer-chain hydrocarbons,

* Corresponding author. E-mail: ishi@tx.technion.ac.il

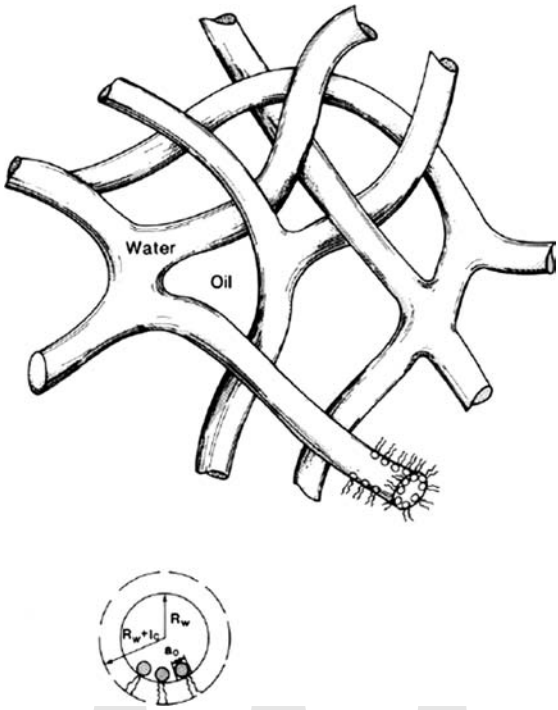

Fig. 1. A model structure proposed by Ninham, Evans and coworkers for a conductive bicontinuous microemulsion formed in low water content water-DDAB-isooctane systems [3].

such as tetradecane, remain conductive even at high water concentrations. Also, the shorter the oil chain, the less water addition was found to be required to reach the abrupt change from conductive to nonconductive behavior [4]. Similar effects have been observed for the viscosity of the system, and for the water self-diffusion coefficient within the microemulsion [5]. This implies that the systems containing small amounts of water are bicontinuous, while the addition of water causes the water phase to become discontinuous.

Ninham, Evans and coworkers [4–6] proposed that the structural change of these microemulsions has to do with changes to the preferred interfacial curvature due to oil penetration into the surfactant tail region. They proposed that the bicontinuous (conductive) microemulsion is made of a network of interconnected cylindrical water conduits within an oil continuum (Fig. 1). The addition of water, they suggested, inflates these conduits, thus decreasing their curvature and the bromide ion concentration within the water phase. Since the tail region of the surfactant is fluid at room temperature, oil intake increases its effective volume, and the preferred curvature of the microemulsion is dictated, among other factors, by the oil used in the microemulsion: smaller oil molecules penetrate better into the tail region, thus leading a higher curvature of inverse structures. For those reasons addition of water causes the transformation of the cylindrical water conduits into smaller, close structures, *i.e.*, spheroidal aggregates, causing the

practical loss of electrical conductivity, and the sharp decrease of water self-diffusion coefficient. In other words, beyond a threshold water concentration, the microemulsion is not bicontinuous any longer, it is oil-continuous, and thus the above-mentioned properties drop by several orders of magnitude.

The DDAB-water-oil system has been investigated extensively. The simple geometric model first presented in 1984 has since been expanded considerably, and DDAB systems have been investigated by various methods [7–10]. However, no direct-imaging mapping of the nanostructure has been performed due to limitations of the available methodologies.

To be able to image nanometric domains, one should use electron microscopy, either transmission electron microscopy (TEM) or scanning electron microscopy (SEM). Both techniques provide at least the supramolecular resolution that is needed for imaging microemulsions. The challenge is to make those systems, which typically have considerable vapor pressure, compatible with the high vacuum of the microscope. In addition, one has to make sure all motion on the supramolecular level is arrested, and that the specimen is thin enough (for TEM) or does not accumulate electric charges (SEM). Also, one has to assure there is sufficient contrast in the prepared specimens, namely, that domains of different composition, *e.g.*, oil and water domains, interact differently with the electron beam. Yet another difficulty of electron microscopy of microemulsions, as of most other complex liquids, or "soft matter" in general, is their high sensitivity to electron radiation-damage, namely destruction of the examined specimen by the electron beam even at very short electron exposures [11].

The goal of direct imaging microemulsions has been elusive. Many microemulsions are notoriously sensitive to small changes of temperature and concentration, as one can see in the many published phase diagrams [12–14], thus the task of preparing electron microscope specimens that preserve the system is not easy. The sensitivity to changes of concentration precludes any preparation techniques that involve an addition of a stain or a fixative. As those stains are typically strong electrolytes, *e.g.*, salts or acids of heavy elements, they are bound to change the ionic strength of the system. Such techniques also involve drying of the specimen, which, again, leads to gradual but drastic change of concentration. Thus to expect nanostructure preservation following such specimen preparation is naïve at best [15]. Capturing the nanostructure at a prescribed temperature is also of utmost importance, another complication of EM specimen preparation of any complex liquid system.

Because of the above-mentioned difficulties, quite early on we chose to take a specimen preparation route based on physical rather than chemical fixation of the specimen [16]. Indeed, cryo-TEM has become almost a standard technique used by many, as can be appreciated from recent review articles [17–19]. Microemulsions have been imaged by cryo-TEM, but they were mostly of the swollen micelle type, *e.g.*, Bernheim-Groswasser *et al.* [20]. Bicontinuous microemulsions have proven to be extremely difficult to image by cryo-TEM due to the very high interfacial surfactant-rich area between oil and water domains, which leads to very high sensitivity to the electron beam. Direct imaging is further complicated by low inherent contrast between the water and oil phases. Another difficulty is that flow-induced nanostructures in microemulsions (MEs) [21] may be formed during cryo-TEM specimen preparation, as documented by [22].

One “classic” study by Jahn and Strey [23] apparently overcame those difficulties by applying another cryo-TEM technique, namely, freeze-fracture-replication (FFR). In that technique a specimen thicker than in the above-mentioned cryo-TEM specimen, is cooled by quenching into a cryogen. It is then fractured, and a metal-carbon replica is prepared of the fracture surface(s). The specimen is then thawed, and the replica is collected and imaged by TEM at room temperature. While Jahn and Strey did a systematic study of several microemulsions, showing the progression of their nanostructure, questions remain regarding the preservation of the native state in the replicas, which were prepared under not fully controlled conditions, and the contrast mechanism, which involved a yet not fully understood surface decoration of the oil domains.

Koetz and coworkers have used cryo-SEM to study a number of different microemulsion systems, *e.g.* [24–26]. However, the methodology and equipment they used made it very difficult to control temperature and concentration of the investigated system. In one publication [26] a systematic direct-imaging study in a given phase diagram was described. Ionic liquid (IL)-based microemulsion were also imaged by cryo-EM. Gao *et al.* [27] used FFR to image their MEs at different compositions and temperature. However, it is not clear how well they were able to control temperature and concentration during specimen preparation. Raba and Koetz [28] used cryo-SEM to image another IL-based ME, but they mention no temperature and concentration control during their specimen preparation, which in the case of the IL-based system may be less crucial. Previously the same group, Rojas *et al.* [29], studied IL-modified MEs by cryo-SEM, but the preservation of nanostructure may not have been good enough.

As part of our long-time interest in the nanostructure of microemulsions, which a long time ago involved also theoretical work [30,31], and our on-going efforts to extend cryo-EM to a wider spectrum of systems, including non-aqueous ones [32,33], we have added cryogenic-temperature scanning electron microscopy (cryo-SEM) to our arsenal of direct imaging methodologies, as a vital complementary technique. Cryo-SEM allows us to image nanometric features in relatively large (micrometer and larger) objects, and image concentrated or highly viscous liquids for which cryo-TEM is not practicable. Recently we described a novel cryo-SEM methodology [34] that allows us prepare specimens under conditions of controlled temperature and concentration, rather similarly to what we have practiced in cryo-TEM for a long time [16]. This methodology allows us image, among others, microemulsion systems.

Using our newly developed cryo-SEM methodology we present here direct imaging of the nanostructure evolution of the DDAB-base microemulsion system described above. This study validates the theoretical model of Ninham and Evans, more than a quarter century after it was suggested.

2. Experimental

Microemulsion preparation was done by weighing proper amounts of DDAB, adding isooctane, and then adding water volumetrically. All solutions showed no apparent macroscopic change for at least a week at room temperature, before being prepared for

microscopy. We chose to study the ternary material system of DDAB, water, and isooctane. We chose isooctane, rather than a normal hydrocarbon, as in the original studies of Ninham and Evans, because branched hydrocarbons do not crystallize even at the relatively slow cooling rates achieved by liquid nitrogen. The cryogen of choice, liquid ethane at its freezing point, cannot be used in this case, as it dissolves the oil [35]. The microemulsions were prepared at constant oil/surfactant weight ratio of 1.5, with increasing amounts of water. A stable single-phase microemulsion was obtained for 20% to 40 wt % water, while a 10 wt % water solution phase-separated into two clear phases, and a 50 wt % water solution phase-separated into a viscous liquid and a gel. All the microemulsions were transparent, and had low viscosity (no quantitative viscosity measurements have been performed so far).

We used didodecyldimethylammonium bromide ($\geq$ 98%) obtained from Fluka, without further purification. Water was purified by a Millipore Milli-Q purification system (conductance $\approx$ 18 m$\mho$). Isooctane (99.5%) was obtained from Carlo Erba.

Cryo-SEM. We prepared cryo-SEM specimens by forming a "sandwich" of a sample drop between two gold planchettes, with a 200 mesh copper grid embedded within the sample. Preparation was carried out in a Controlled Environment Vitrification System (CEVS) in a fully controlled saturation and temperature environment. Details of this modified CEVS and the methodology of specimen preparation are given elsewhere [34]. The CEVS chamber was saturated with water and isooctane in equal amounts. For all samples, preparation was performed at 25 °C.

We vitrified the specimens by plunging them into liquid nitrogen. The cooling rates achieved by liquid nitrogen are insufficient to vitrify the water domains. However, as those domains are rather small, tens of nanometers at the most in at least two dimensions, their freezing does not lead to nanostrucutral changes. We have shown that recently by cryo-TEM in a study of high internal phase microemulsions [36]. We fractured and coated the specimens with a 4 nm carbon/platinum layer in a Bal-Tec BAF 060 system. Specimens were then transferred into the scanning electron microscope using a Bal-Tec VCT100 cryo-transfer system. Imaging was performed in a Zeiss Ultra Plus high-resolution scanning electron microscope equipped a field-emission gun, and fitted with a VCT100 cold-stage system. We imaged the samples at temperatures below −140 °C. We operated the microscope at accelerating voltage of 1 kV to achieve high resolution. Imaging was done with two secondary electron detectors: an Everhart–Thornley detector and a high-resolution in-the-column detector.

3. Results and discussion

To the best of our knowledge ternary DDAB microemulsions including a branched hydrocarbon as the oil have not been investigated yet. However, the basic prediction of a bicontinuous structure for low water content is independent of the oil. That is supported by NMR self-diffusion measurements [5], suggesting a bicontinuous structure for all oils that form microemulsions with DDAB and water, those that penetrate either well or poorly into the surfactant tail domains of the oil-water interfacial region. The main effect of the oil type is in determining at what point the structural transition from bicontinuous to oil-continuous structure occurs. Given that the main chain of isooctane

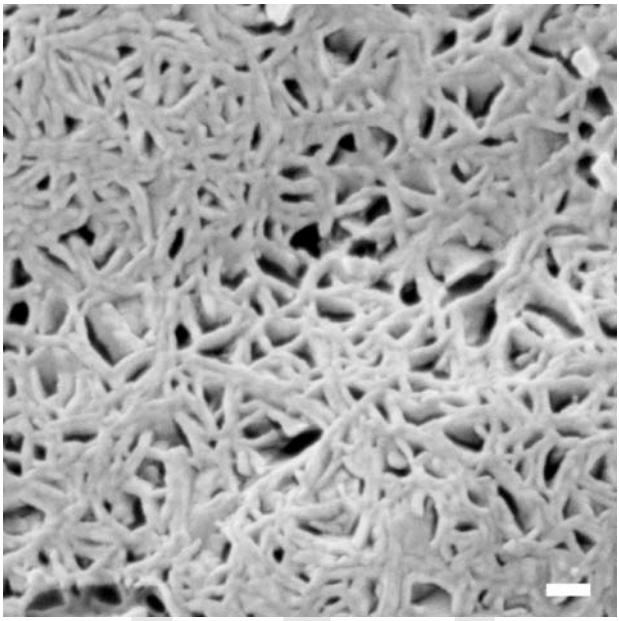

Fig. 2. A cryo-SEM micrograph of a 48%/32%/20 wt% isooctane/DDAB/water microemulsion; bar = 100 nm.

consists of 5 carbon atoms, and that its branches are short, even without detailed theoretical analysis one could expect that such a transition should occur. This expectation is verified by our experimental results, shown below.

Figure 2 is a cryo-SEM micrograph of a 48%/32%/20 wt% isooctane/DDAB/water system, which was the lowest water content system investigated. It shows a network structure, as predicted for low water content microemulsions. The lighter domains of the image are inverse swollen threadlike (cylindrical) micelles water conduits, about 20–30 nm in diameter, interconnected into a network. The structure we observe directly by our novel methodology is strikingly similar to the model cartoon suggested over 25 yr ago by Chen *et al.* [3] (Fig. 1).

The excellent contrast we obtained in Fig. 2 and in other cryo-SEM images of this system requires some discussion. It is peculiar that the water domains are very bright, while the isooctane surrounding them appears as dark domains in those micrographs. This contrast is explained after we consider the vapor pressure of water and isooctane at cryogenic temperatures. As seen in Fig. 3, while around ambient temperature isooctane and water have similar vapor pressure, at cryogenic temperature water vapor pressure drops to very low values, while isooctane retains vapor pressure levels, which are high enough to give sufficient sublimation rates that leave empty domains previously filled with isooctane. For comparison, the pressure in the specimen chamber of our SEM was around 2×10^{-6} mbar. In fact, one can actually follow that sublimation process while examining the cryo-specimens in the SEM [37], even under low electron exposure. Thus, the very good contrast in micrographs, *e.g.*, Fig. 2, is due to high emission

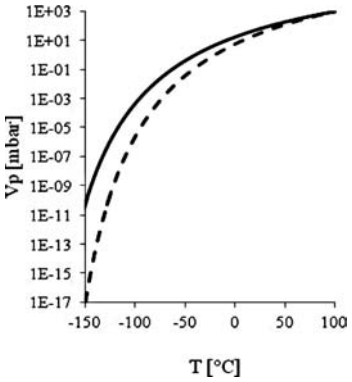

Fig. 3. Comparison of vapor pressures of water (dashed line) and isooctane (solid line) at cryogenic temperatures, as calculated according to the Antoine equation. It can be seen that at low temperatures, the vapor pressure of isooctane is several orders of magnitude higher than that of water. Note that Antoine constants used for isooctane are valid only for temperatures going down to about −70 °C [38,39], but the vapor pressure separation trend is clearly apparent even at that temperature.

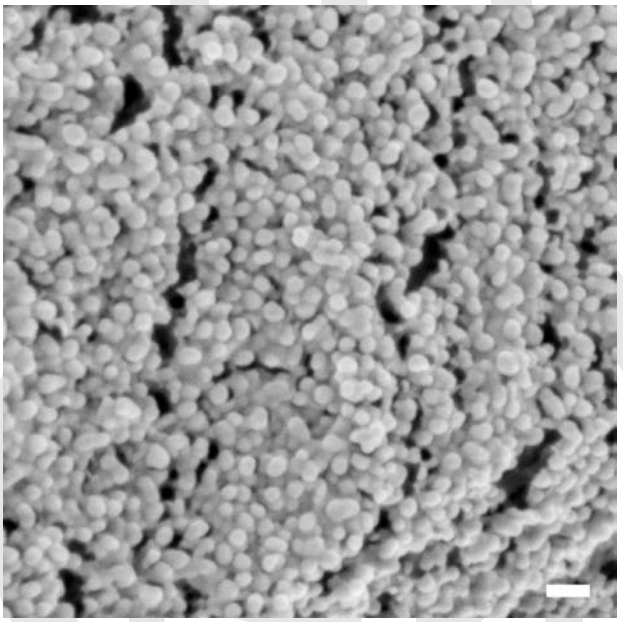

Fig. 4. A cryo-SEM micrograph of a 36%/24%/40 wt % isooctane/DDAB/water microemulsion; bar = 100 nm.

of secondary electron from the water domains, compared to no emission for the cavities, previously filled with isooctane.

The most water-rich microemulsion we investigated in this study consisted of 36%/24%/40 wt % isooctane/DDAB/water. In this case we observed spherical and

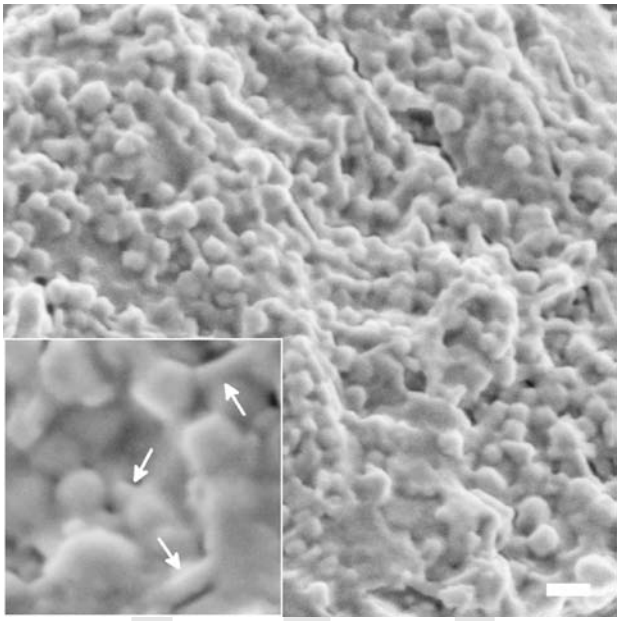

Fig. 5. A cryo-SEM micrograph of a 42%/28%/30 wt % isooctane/DDAB/water microemulsion; bar = 100 nm. Inset – doubled magnification. Arrows indicate conduits connecting inverse swollen micelles.

slightly elongated inverse swollen micelles, about 30–50 nm in diameter (Fig. 4), in agreement with previous investigation by dynamic light scattering and flow birefringence [10]. Such an oil-continuous system should have very poor electrical conductivity, as originally reported and explained a long time ago. In this case, too, the system is directly-imaged here for the first time. That we image so clearly the swollen micelles, is, again, the result of the differential sublimation of the surrounding isooctane of the thermally-fixed system.

Now we turn our attention to a microemulsion system of an intermediate water content, namely, 42%/28%/30 wt % isooctane/DDAB/water. Figure 5 shows that the nanostructure of this system is indeed an intermediate between the two previous systems. It, too, is made of inverse swollen micelles. As before, contrast was enhanced by differential isooctane sublimation. However, those micelles are larger, with diameters in the 50–75 nm range. Many of those are connected by "conduits", which are rather similar to those we observed in the bicontinuous electrically conductive, relatively water-poor system, where the diameters were in the 25 to 35 nm range. The insert in Fig. 5 shows quite clearly the spheroidal micelles fused into threadlike micelles.

These results illustrate structural evolution that may be qualitatively explained as the result of a balance between two factors. While the penetration of oil into the hydrophobic domains and bromide ion concentration dictate an optimal curvature, the total water-oil interfacial area is dictated by surfactant concentration. At very low water content, bromide ion concentration in the water and surfactant content are high, thus small-diameter network of conduits of water (branched, interconnected threadlike mi-

celles) are formed. Addition of water dilutes the aqueous bromide ion concentration, and is expected to decrease structural (absolute) curvature by less effectively screening headgroup repulsion within the water phase in the inverse aggregates. This is accomplished by the formation of larger-radius inverse spherical micelles, and, perhaps, by the increase in the radius of water conduits as well. The decrease in interfacial area is caused by the geometric fact that the surface area-to-volume ratio is proportional to $1/d$, where d is a characteristic diameter. Note also that the variation of volume for spheres is stronger than the variation of volume for cylinders with regards to diameter, making it reasonable to assume that oil intake in the tail region is more significant for the spheroidal micellar structure than for the network structure (for a similar headgroup areas in both structures). This may partially explain the observation that larger inverse micelles form in the oil-continuous phase.

In summary, our cryo-SEM methodology, based on carefully controlled specimen preparation and state-of-the-art equipment, has proven to be most useful for the direct nanostructural characterization of microemulsions systems, some of the most elusive liquid systems, given their very high sensitivity to concentration and temperature changes. We were able to image the bicontinuous network structure formed at low water content microemulsions, and the oil continuous phase at higher water content. We were also able to capture the intermediate nanostructure between the bicontinuous and the oil-continuous phase. This nanostrucutral evolution agrees with theoretical predictions based on a geometric model presented by Ninham, Evans, and coworkers in 1984. Our results indicate that slight changes in structural curvature may occur throughout the single-phase microemulsion region to accommodate the compositional change of the solution, as well as geometric requirements imposed by the surfactant.

Acknowledgement

We thank Na'ama Koifman, Liron Issman, Dr. Ellina Kesselman, and Berta Shdemati for their help in conducting experiments, and for fruitful discussion. Liron Issman provided Fig. 3. The Israel Science Foundation (ISF) and the Technion Russell Berrie Nanotechnology Institute (RBNI) have given partial financial support for this work.

References

1. L. R. Angel, D. F. Evans, and B. W. Ninham, J. Phys. Chem. **87** (1983) 538.
2. B. W. Ninham, S. J. Chen, and D. F. Evans, J. Phys. Chem. **88** (1984) 5855.
3. S. J. Chen, D. F. Evans, B. W. Ninham, D. J. Mitchell, F. D. Blum, and S. J. Pickup, J. Phys. Chem. **90** (1986) 842.
4. S. J. Chen, D. F. Evans, and B. W. Ninham, J. Phys. Chem. **88** (1984) 1631.
5. F. D. Blum, S. Pickup, B. W. Ninham, S. J. Chen, and D. F. Evans, J. Phys. Chem. **89** (1985) 711.
6. F. E. Evans and H. Wennerström, *The Colloidal Domain*, 2nd ed., VCH, New York (1999).
7. K. Fontell, A. Ceglie, B. Lindman, and B. Ninham, Acta Chem. Scand. **A40** (1986) 247.
8. V. Chen, G. G. Warr, D. F. Evans, and F. G. Prendergast, J. Phys. Chem. **92** (1988) 768.
9. I. S. Barnes, S. T. Hyde, B. W. Ninham, P. J. Derian, M. Drifford, and T. N. Zemb, J. Phys. Chem. **92** (1988) 2286.
10. U. Lenz and H. Hoffmann, Ber. Bunsen. Phys. Chem. **96** (1992) 809.
11. Y. Talmon, M. Adrian, and J. Dubochet, J. Microsc. **141** (1986) 375.

12. H. Kunieda and K. Shinoda, J. Dispers. Sci. Technol. **3** (1982) 233.
13. U. Olsson, K. Shinoda, and B. Lindman, J. Phys. Chem. **90** (1986) 4083.
14. M. Kahlweit and R. Strey, J. Phys. Chem. **90** (1986) 5239.
15. Y. Talmon, J. Colloid Interface Sci. **93** (1983) 366.
16. J. R. Bellare, H. T. Davis, L. E. Scriven, and Y. Talmon, J. Electron Microsc. Tech. **10** (1988) 87.
17. Y. Talmon, *Seeing* Giant Micelles Cryogenic-Temperature Transmission Electron Microscopy (Cryo-TEM), in: *Giant Micelles*, R. Zana, E. A. Kaler (Ed.), CRC Press, New York (2007).
18. H. Cui, T. K. Hodgdon, E. W. Kaler, L. Abezgauz, D. Danino, M. Lubovsky, Y. Talmon, and D. J. Pochan, Soft Matter **3** (2007) 945.
19. S. Zhong and D. J. Pochan, Polym. Rev. **50** (2010) 287.
20. A. Bernheim-Groswasser, T. Tlusty, S. A. Safran, and Y. Talmon, Langmuir **15** (1999) 5448.
21. G. Gonnella and M. Ruggieri, Phys. Rev. E **66** (2002) 3150.
22. Y. Zheng, Z. Lin, J. L. Zakin, Y. Talmon, H. T. Davis, and L. E. Scriven, J. Phys. Chem. B **104** (2000) 5263.
23. W. Jahn and R. Strey, J. Phys. Chem. **92** (1988) 2294.
24. S. Lutter, B. Tiersch, J. Koetz, A. Boschetti-de-Fierro, and V. Abetz, J. Colloid Interface Sci. **311** (2007) 447.
25. C. Note, J. Ruffin, B. Tiersch, and J. Koetz, J. Dispers. Sci. Technol. **28** (2007) 155.
26. S. Lutter, J. Koetz, B. Tiersch, and S. Kosmella, J. Dispers. Sci. Technol. **30** (2009) 745.
27. Y. Gao, N. Li, L. Hilfert, S. Zhang, L. Zheng, and L. Yu, Langmuir **25** (2009) 1360.
28. C. Rabe and J. Koetz, Colloids Surf. A **354** (2010) 261.
29. O. Rojas, J. Koetz, S. Kosmella, B. Tiersch, P. Wacker, and M. Kramer, J. Colloid Interface Sci. **333** (2009) 782.
30. Y. Talmon and S. Prager, Nature **267** (1977) 333.
31. Y. Talmon and S. Prager, J. Phys. Chem. **69** (1978) 2984.
32. D. Danino, R. Gupta, J., Satyavolu, and Y. Talmon, J. Colloid Interface Sci. **249** (2002) 180.
33. A. N. G. Parra-Vasquez, N. Behabtu, M. Green, C. Pint, C. Young, J. Schmidt, E. Kesselman, A. Goyal, P. Ajayan, Y. Cohen, Y. Talmon, R. H. Hauge, and M. Pasquali, ACS Nano **4** (2010) 3969.
34. L. Issman and Y. Talmon, J. Microsc. **246** (2012) 60.
35. Y. Talmon, Cryogenic Temperature Transmission Electron Microscopy in the Study of Surfactant Systems, in: *Modern Characterization Methods of Surfactant Systems*, B. P. Binks (Ed.), Surfactant Science Series, Marcel Dekker, New York (1999).
36. L. Wolf, H. Hoffmann, T. Teshigawara, T. Okamoto, and Y. Talmon, J. Phys. Chem. B **116**, (2012) 2131.
37. N. Koifman, M.Sc. dissertation, Technion-Israel Institute of Technology, Haifa, Israel (2012).
38. G. Milazzo, Ann. Chim. Rome **46** (1956) 1105.
39. D. R. Stull, Ind. Eng. Chem. **39** (1947) 517.